Collision-induced rotational excitation in $N_2^+(^2\Sigma_g^+, v=0)$–Ar: Comparison of computations and experiment

Oliver T. Unke, Juan Carlos Castro-Palacio', Raymond J. Bemish, and Markus Meuwly'

Citation: J. Chem. Phys. **144**, 224307 (2016); doi: 10.1063/1.4951697
View online: http://dx.doi.org/10.1063/1.4951697
View Table of Contents: http://aip.scitation.org/toc/jcp/144/22
Published by the American Institute of Physics

Collision-induced rotational excitation in $N_2^+(^2\Sigma_g^+, v = 0)$–Ar: Comparison of computations and experiment

Oliver T. Unke,[1] Juan Carlos Castro-Palacio,[1,a)] Raymond J. Bemish,[2] and Markus Meuwly[1,b)]
[1]*Department of Chemistry, University of Basel, Klingelbergstrasse 80, CH-4056 Basel, Switzerland*
[2]*Air Force Research Laboratory, Space Vehicles Directorate, Kirtland AFB, New Mexico 87117, USA*

(Received 14 February 2016; accepted 9 May 2016; published online 13 June 2016)

The collisional dynamics of $N_2^+(^2\Sigma_g^+)$ cations with Ar atoms is studied using quasi-classical simulations. N_2^+–Ar is a proxy to study cooling of molecular ions and interesting in its own right for molecule-to-atom charge transfer reactions. An accurate potential energy surface (PES) is constructed from a reproducing kernel Hilbert space (RKHS) interpolation based on high-level *ab initio* data. The global PES including the asymptotics is fully treated within the realm of RKHS. From several ten thousand trajectories, the final state distribution of the rotational quantum number of N_2^+ after collision with Ar is determined. Contrary to the interpretation of previous experiments which indicate that up to 98% of collisions are elastic and conserve the quantum state, the present simulations find a considerably larger number of inelastic collisions which supports more recent findings. *Published by AIP Publishing.* [http://dx.doi.org/10.1063/1.4951697]

I. INTRODUCTION

Cooling neutral and charged atoms and molecules is essential for controlled investigations of fundamental processes in chemistry and physics. These methods rely in one way or another on the energy transfer between the species to be cooled and their environment. Many techniques to achieve cooling to the millikelvin regime exist. They include, among others, sympathetic cooling of neutral atoms through collisions with laser-cooled species[1] or cooling through collisions with Ar atoms in crossed molecular beams.[2]

An ionic system which is of considerable interest in this context is N_2^+–Ar. It is a prototypical system to study molecular ions[3,4] and charge transfer reactions for different internal states of the diatomic.[5] Previous experiments showed that charge transfer from the molecule to the atom occurs only if N_2^+ is vibrationally excited and no charge transfer is possible for $N_2^+(v'' = 0)$.[3] Figure 1 shows relevant stages for the $N_2^+(v'', j'') + Ar \rightarrow N_2(v', j') + Ar^+$ reaction.

Another process which takes place on the electronic ground state potential energy surface (PES) is scattering of the Ar atom from the cation through formation of the collision complex $[N_2Ar]^+$ (right hand side in Figure 1). Recent experiments of sympathetically cooled $N_2^+(v = 0, N = 0, J = 0.5)$ and collisions with room temperature Ar atoms have shown that the measured rate for quadrupole vibrational excitation of N_2^+ in Coulomb crystals is two orders of magnitude lower than expected.[9] It was speculated that this is due to depopulation of the initially prepared molecular state through rotationally inelastic collisions between the N_2^+ ion and the Ar buffer gas. This process has been previously investigated using laser excited N_2^+ in a 22-pole ion trap in the presence of a low density Ar buffer at 90 K. Specifically, the rotational state $J = 6.5$ of a small number of N_2^+ ions was depopulated via laser induced charge transfer with subsequent observation of refilling the hole via inelastic collisions. Analysis of the experimental data using an advanced kinetic model yields a very low inelastic collision rate ($\leq$2%).[3] In order to address these conflicting experimental results and to provide a more atomistically resolved picture, it is desirable to investigate this system using accurate computations. Such an approach has provided further insight into related elementary processes including, e.g., the rotational excitation of N_2^+ through collisions with N_2[10] and the reactive collisions of NO + O[11,12] and OH + H.[13]

The present work focusses on the final state distribution of the rotational quantum number j' of the N_2^+ ion after collision with Ar starting from a given initial rotational state j'' (right hand side in Figure 1). Such simulations provide information about the conservation of the internal state of N_2^+ during and after collisions. Because of the appreciable binding energy of 1.14 eV stabilizing the $[N_2Ar]^+$ complex (see Figure 1), it is expected that the dynamics in the bound state $[N_2Ar]^+$ lead to inelastic collisions and give rise to rotational excitation. Earlier experimental results suggest the contrary, namely, that rotational transitions in N_2^+ + Ar collisions occur rarely and up to 98% are elastic ("...implies that only one out of 50 collisions results in a change of the rotational state").[3] A possible explanation for the surprising conservation of the initial rotational state could be the consequence of some hidden constants of motion leading to approximate selection rules.[3]

The collision of N_2^+ molecules with Ar atoms is studied through quasi-classical molecular dynamics (MD) simulations. Hence, quantum effects due to zero-point vibrations and tunneling, which may influence the collisional dynamics and the resulting rotational excitation of N_2^+, are not

a)Current address: Department of Earth Sciences & Engineering, Imperial College of London, Exhibition Road, London SW7 2AZ.
b)m.meuwly@unibas.ch

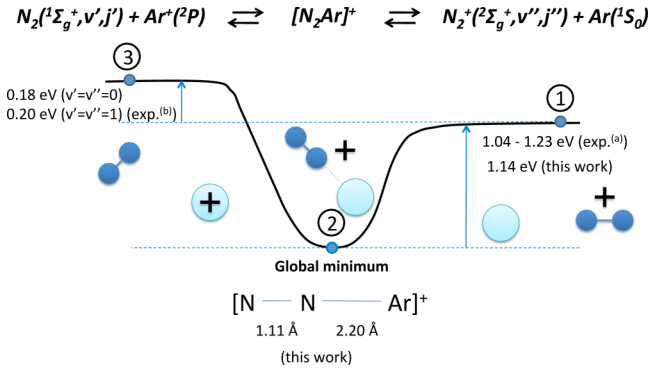

FIG. 1. Schematic representation of the relevant stages in the $N_2(v',j') + Ar^+ \rightarrow N_2^+(v'',j'') + Ar$ reaction. Experimentally determined values are indicated by "exp" where the superscript (a) refers to Ref. 6 and (b) to Refs. 7 and 8. For the vibrational and rotational ground state, the $N_2^+(v'',j'') + Ar$ channel is 0.179 eV below the $N_2(v',j') + Ar^+$ asymptote.[7,8] The reported experimental dissociation energy of the $[N_2Ar]^+$ complex ranges from 1.04 to 1.23 eV.[6] In this work, the process studied is $N_2^+(0,j'') + Ar \rightarrow N_2^+(0,j') + Ar$.

included in the simulations. Moreover, rotational fine structure originating from coupling of the spin of N_2^+ and the angular momentum of the diatomic is not included in the present approach. Accurate full close-coupling quantum scattering calculations even for triatomic systems with a deep well (here in excess of 1 eV), a highly anisotropic interaction potential, and a small rotational constant for the diatomic are currently not feasible.[14] On the other hand, quasi-classical trajectory (QCT) simulations have provided valuable insight into rotational excitation in the charge exchange reaction $N_2^+ + N_2 \rightarrow N_2 + N_2^+$.[10] Similar classical studies have been performed for the $O + CHD_3$ system[15] and rates of the hydrogen exchange reaction $OH^- + HBr \rightarrow Br^- + H_2O$ (down to 5 K with experimental data available for 20 K and up) without accounting for spin-orbit coupling (as in the present case) and still, good agreement with experiment was obtained.[16] State-to-state dynamics of the $Br + H_2$ reaction based on QCT calculations was found to reproduce the quantum mechanical results in general terms (e.g., for state-to-state excitation functions) although sometimes the agreement was only qualitative.[17] However, in the light of the computational demands of a fully quantum mechanical treatment (see above) and the aforementioned insights obtained for similar systems, a classical treatment appears to be a meaningful approach. To further assess the role of quantum effects, the classical results are complemented with calculations accounting for quantum zero point energy (ZPE) using two different methods.

The ZPE motion of N_2^+ may have non-negligible effects on the results. In particular, since all simulations are carried out within the framework of classical mechanics, ZPE might be consumed and lead to excitation of internal degrees of freedom, which is unphysical. Since there is no unique way to correct for ZPE,[18] two different strategies to probe this are explored: (a) trajectories are run on the bare, *ab initio* PES and a binning criterion is applied at the analysis stage, and (b) the trajectories are run on a ZPE-corrected PES in order to prevent the unphysical consumption of ZPE during the simulations. Both a binning criterion[19] and a way to constrain vibrational motion[20,21] have been previously employed in the literature. The PES is constructed from *ab initio* points using interpolation by the reproducing kernel Hilbert space (RKHS) formalism.[22,23] Since the present work focuses on the study of rotational transitions in $N_2^+(v'' = 0, j'') + Ar$ collisions, only the electronic ground state of N_2^+ is considered.

II. METHODS

A. *Ab initio* calculations

The N_2^+–Ar system is described in Jacobi coordinates, where r is the N–N distance, R is the distance between Ar and the center of mass of the nitrogen atoms, and α is the angle between the direction of R and the N–N axis (see Figure 2).

A total of 3025 points on a regular grid were used to sample the PES at the unrestricted coupled cluster single double (triple) (UCCSD(T)) level of theory with an aug-cc-pVTZ basis set[24,25] using the Gaussian 09 suite of codes.[26] The angular grid corresponds to an 11-point Gauss-Legendre quadrature (α = 11.815°, 27.452°, 43.089°, 58.726°, 74.363°, 90.000°, 105.637°, 121.274°, 136.911°, 152 548°, 168.185°).[27] For r, the grid consists of 11 points according to the equilibrium position r_{eq} of the N_2^+ bond and the turning points[28] from $v = 0$ to $v = 4$ (r = 0.998, 1.010, 1.024, 1.043, 1.071, 1.122, 1.167, 1.207, 1.237, 1.263, 1.287 Å). The grid of van der Waals distances R was chosen to capture the well-region with more densely spaced points and the asymptotic regions with fewer points, for a total of 25 radial grid points (R = 1.7, 1.8, 1.9, 2.0, 2.1, 2.2, 2.3, 2.4, 2.5, 2.6, 2.7, 2.8, 2.9, 3.0, 3.1, 3.2, 3.3, 3.4, 3.5, 3.6, 3.8, 4.1, 4.5, 6.0, 9.0 Å).

The geometry of the $[N_2Ar]^+$ complex was optimized and the most stable configuration was found to be linear with Jacobi coordinates of the optimized structure of r_{eq} = 1.105 Å, R_{eq} = 2.749 Å, and α_{eq} = 0°. The dissociation energy D_e of the complex in the linear configuration is 1.266 eV with a zero point energy of 0.129 eV (calculated at the UCCSD(T)/aug-cc-pVTZ level of theory). Thus the dissociation energy D_0

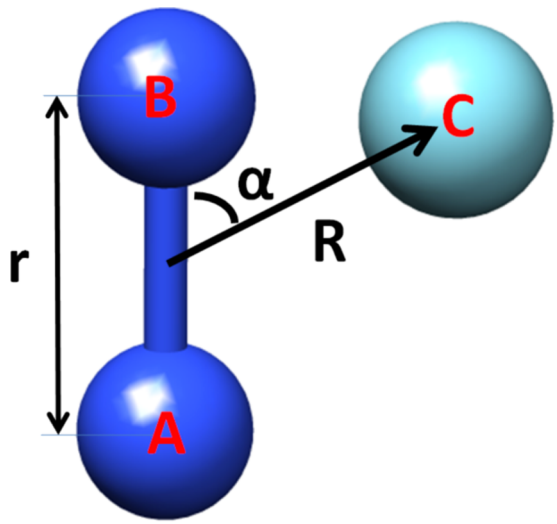

FIG. 2. $N_2^+ + Ar$ system described in Jacobi coordinates. The dark blue spheres A and B correspond to the nitrogen atoms and the light blue sphere C to the argon atom.

of 1.137 eV is in good agreement with the experimentally measured value of 1.109 eV.[29]

B. RKHS interpolation

In the following, only a description of the RKHS formalism is provided for completeness. For more details, the reader is referred to the literature.[30]

1. General procedure

For constructing a multi-dimensional representation of a PES $V(\mathbf{x})$ for a molecular system based on N *ab initio* data points at an arbitrary configuration $\mathbf{x}$, $V(\mathbf{x})$ is considered to be a bounded function. The quality of the representation of $V(\mathbf{x})$ in terms of a kernel is determined by two aspects: one is the number of grid points which equals the number of kernel coefficients that are used, and the other is the type of kernel function itself. As such, $V(\mathbf{x})$ can be represented in the following fashion:

$$V(\mathbf{x}) = \sum_{i=1}^{N} w_i Q(\mathbf{x}_i, \mathbf{x}), \tag{1}$$

where $\mathbf{x}_i$ are the coordinates of the system at the ith grid point, w_i are the kernel coefficients, and $Q(\mathbf{x}_i, \mathbf{x})$ is a reproducing kernel.

The multidimensional reproducing kernel $Q(\mathbf{x}, \mathbf{x}')$ can be represented as a product over 1-dimensional kernels.[30] For example, if $\mathbf{x}$ corresponds to the Jacobi coordinates (r, R, α), the 3-dimensional kernel can be expressed as

$$Q(\mathbf{x}, \mathbf{x}') = q_1(r, r') \cdot q_2(R, R') \cdot q_3(\alpha, \alpha'), \tag{2}$$

where the kernels q_i can be chosen freely depending on the nature of the respective variable (angular or distance-like). The kernel coefficients w_i in Eq. (1) are determined by solving the following system of linear equations:

$$\begin{bmatrix} Q(\mathbf{x}_1,\mathbf{x}_1) & Q(\mathbf{x}_1,\mathbf{x}_2) & \cdots & Q(\mathbf{x}_1,\mathbf{x}_N) \\ Q(\mathbf{x}_2,\mathbf{x}_1) & Q(\mathbf{x}_2,\mathbf{x}_2) & \cdots & Q(\mathbf{x}_2,\mathbf{x}_N) \\ \vdots & \vdots & \ddots & \vdots \\ Q(\mathbf{x}_N,\mathbf{x}_1) & Q(\mathbf{x}_N,\mathbf{x}_2) & \cdots & Q(\mathbf{x}_N,\mathbf{x}_N) \end{bmatrix} \begin{bmatrix} w_1 \\ w_2 \\ \vdots \\ w_N \end{bmatrix} = \begin{bmatrix} V^{ab\ initio}(\mathbf{x}_1) \\ V^{ab\ initio}(\mathbf{x}_2) \\ \vdots \\ V^{ab\ initio}(\mathbf{x}_N) \end{bmatrix}. \tag{3}$$

Since the reproducing kernel matrix is symmetric and positive definite by definition, the computationally efficient Cholesky decomposition can be used to solve Eq. (3).[31] Once the kernel coefficients w_i are known, the energy at an off-grid point $\mathbf{x}$ can be evaluated from Eq. (1).

2. 1-dimensional kernels

Distance-like coordinates. In this work, the 1-dimensional kernel for distance-like coordinates was that from Ref. 30,

$$q^{n,m}(x, x') = n^2 x_>^{-(m+1)} B(m+1, n) \times {}_2F_1(-n+1, m+1; n+m+1; \frac{x_<}{x_>}), \tag{4}$$

where $B(m+1,n)$ is the beta function, ${}_2F_1(-n+1, m+1; n+m+1; x_</x_>)$ is the Gauss hypergeometric function, and $x_<$ and $x_>$ denote the smaller and the larger of x and x', respectively. The chosen value for n controls up to which derivative the kernel is smooth, while the value of m controls its long-range behaviour.[30] In particular, if no points are available in the asymptotic region, m can be chosen to mimic the physical long-range behaviour of the interpolated variable. Here we use $n = 2$ and $m = 6$ for both distance-like kernels, although different values are possible.[32] In the present work, the choice of m is largely inconsequential because enough data are available in asymptotic regions and the *ab initio* points are necessarily reproduced exactly.

Angle-like coordinates. For angle-like internal coordinates, the general expression for the kernel is[30]

$$q^n(x, x') = \sum_{i=0}^{n-1} x_>^i x_<^i + n x_<^n x_>^{n-1} {}_2F_1(1, -n+1; n+1; \frac{x_<}{x_>}). \tag{5}$$

Eq. (5) is valid only if the angle-like coordinate is rescaled so that both x and x' belong to the interval $[0, 1]$. For example, to rescale the Jacobi coordinate α, a new coordinate y is defined as $y = (1 - \cos\alpha)/2$. Again, choosing $n = 2$ is sufficient for an accurate representation of the angular dependence.

3. Treatment of the asymptotics

The 1-dimensional distance-like kernel given by Eq. (4) has the advantage that it correctly decays to zero at long range. While this is still true in the present case for one particular value of the N–N separation r, this is not the case for the total energy of the complex for arbitrary values of r. The correction of the asymptotics was considered in previous work on HO_2 by using a manybody expansion of the PES.[33] For the present work, a different method, which is fully within the RKHS formalism, was used and is presented in Section III A.

Correction of ZPE in the N_2^+–Ar *PES*. One way to account for ZPE in the simulations is to carry out a point-wise correction of the PES whereby the ZPE contribution is taken into account at each configuration.[34] This contribution is calculated from the harmonic oscillator energy evaluated for $n = 0$,

$$V^{ZPE} = \sum_{i=1}^{N} \left(\frac{1}{2} + n\right) \hbar\omega_i, \tag{6}$$

where $N = 3$ is the number of degrees of freedom of the system and ω_i are the positive eigenvalues obtained from *ab initio* calculations at the MP2/aug-cc-pVTZ level of theory.

In the present simulations, two different PESs were employed, one where the ZPE correction given by Eq. (6) is included (*ZPE-corrected PES*) and one where no such correction was made (*bare PES*). The RKHS PES and its quality compared to off-grid points are shown in Figure 3.

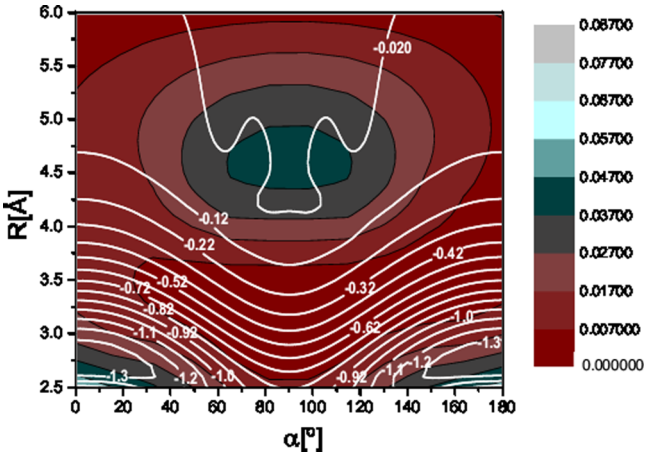

FIG. 3. Contour plot of the RKHS interpolated N_2^+–Ar PES (white lines) with N_2^+ at its equilibrium position ($r_{eq} = 1.122$ Å). The binding energy is around 1.3 eV and isocontours are labelled with energies in eV. The color map is the error surface with relative errors in %. Relative errors were obtained by comparing the interpolated energies to off-grid *ab initio* data. Even the largest relative errors are below 0.1%.

C. Molecular dynamics simulations

MD simulations of the collision between N_2^+ and Ar have been carried out with CHARMM.[35] The equations of motion were integrated using a time step of $\Delta t = 0.1$ fs and energies were calculated from the RKHS representation of the PES described in Section II B using the bare and ZPE-corrected PESs, respectively. Forces were obtained by numerical differentiation using a five-point stencil.[36]

Initial conditions were generated from a WKB-quantized periodic orbit of the corresponding rotating Morse oscillator for given vibrational v and rotational j quantum numbers.[37,38] Parameters for the Morse potential were fitted to *ab initio* data for N_2^+ ($D_e = 8.5003$ eV, $r_e = 1.1307$ Å, $\beta = 2.5928$ Å $^{-1}$). The fitted dissociation energy is consistent with the experimental value of 8.724 eV.[39] The initial vibrational quantum number was $v'' = 0$ and the rotational quantum numbers were either $j'' = 0$ or $j'' = 6$. Relative collision energies between N_2^+ and Ar were sampled from a Maxwell-Boltzmann distribution at either 90 K or 300 K. These initial conditions are representative of the previous experiments which investigate $[N_2^+(v'' = 0, j'' = 6);\ T = 90\ \text{K}]$[3] and the collision of ultracold molecular ions with Ar at room temperature $[N_2^+(v'' = 0, j'' = 0);\ T = 300\ \text{K}]$.[9] The impact parameter b was selected from a uniform distribution between 0 and 25 a_0 (prior test runs had shown that larger impact parameters do not lead to collision or even mutual influence of the impact partners). Such a procedure was already employed in previous studies of the collisions between $O(^3P)$ and $NO(^2\Pi)$.[11]

Simulations on the ZPE-corrected PES used a suitably modified procedure for generating initial conditions for the positions and velocities. For $v'' = 0$ and any j'', the position is always set to the minimum of the effective Morse potential $V_{\text{eff}}(r) = V(r) - \frac{j''(j''+1)}{r^2}$ and all vibrational energies are removed from the N–N stretch as the ZPE is already accounted for in the corrected PES. The vibrational energy corresponding to the ZPE is added back prior to the analysis in order to be able to use the same filtering criteria for the ZPE-corrected and bare PES.

All trajectories were run until the collision partners were fully separated for which a value corresponding to more than 1.3-times their initial separation was assumed. The maximum simulation time considered was 1 ns. For statistically significant results, a total of 25 000 trajectories were run for each temperature and PES and approximately 4000 of them were excluded from the analysis due to lifetimes longer than 1 ns.

III. RESULTS

A. Correction of the asymptote

Depending on the N_2^+ bond length r, individual manifolds $V(R, \alpha; r)$ dissociate to different asymptotic values for $R \to \infty$. This assumes that the PES becomes isotropic (α–independent) with increasing R which is in general true. In order to employ RKHS interpolation in a meaningful fashion for the R– and α–degrees of freedom, the asymptotic value for each manifold characterized by a specific value for the N–N separation must be shifted to zero energy. This is necessary because kernels decay to zero asymptotically (Fig. 4).

In order to set the energy to zero for every cut (r = constant), the energy of the isolated diatomic $E(r, R \to \infty)$ is subtracted from the energy of all points that share the same value of r and yields $V^{\text{new}}(r, R, \alpha) = E(r, R, \alpha) - E(r, R \to \infty)$ and $V^{\infty}(r) = E(r, R \to \infty)$. The two data sets $V^{\text{new}}(r, R, \alpha)$ and $V^{\infty}(r)$ are then interpolated within the RKHS framework. Because the PES is isotropic for sufficiently large R, the interpolation of $V^{\infty}(r)$ requires only a 1-dimensional kernel. Hence, all quantities required are represented by

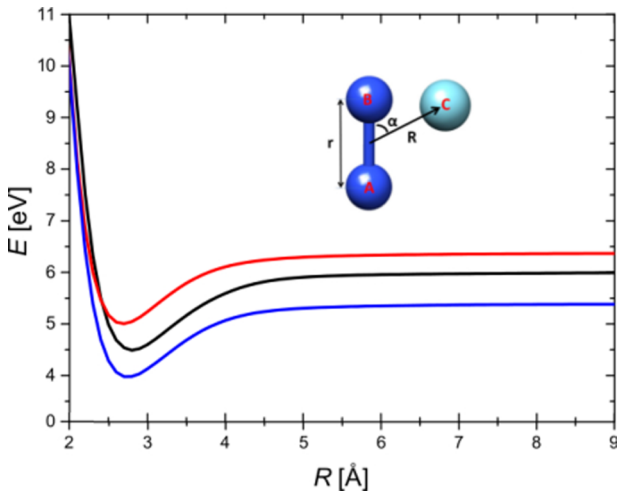

FIG. 4. Part of the global PES for a triatomic system N_2^+–Ar. The relevant coordinates (r, R, α) are indicated in the inset with the dark blue spheres corresponding to the N_2^+ molecule and the light blue sphere to the Ar atom. The three curves refer to different intermolecular distances of the diatomic N_2^+ (r_{NN}), $r_{\text{NN}} = 1.00$ Å (red), $r_{\text{NN}} = 1.11$ Å (blue), and $r_{\text{NN}} = 1.21$ Å (black). In the quantum chemistry calculations, the asymptotes of each manifold characterized by the particular r_{NN} separation dissociate to its own asymptote as indicated by the non-overlapping curves at long range. If the asymptote is not corrected in the RKHS interpolation, all curves converge to a value of $E = 0$ for large R.

kernels and the global PES can be evaluated at an off-grid point (r^0, R^0, α^0) according to Eq. (7),

$$V(r^0, R^0, \alpha^0) = V^{\text{new}}(r^0, R^0, \alpha^0) + V^{\infty}(r^0). \quad (7)$$

B. Simulation and analysis of collisional excitation

Simulations on the bare and ZPE-corrected PES were carried out with a range of initial conditions. The physical conditions included two temperatures: $T = 90$ K and $T = 300$ K. The first corresponds to previous experiments[3] and the latter was chosen to examine the role of temperature on the results. The time step in all simulations was $\Delta t = 0.1$ fs. Overall, 25 000 trajectories were run for each temperature. However, a considerable number of trajectories are not further analyzed because they violate in one way or another restrictions imposed by quantum mechanics. Such filtering at the post-processing stage is a usual procedure to limit the number of classical trajectories to be analyzed to those which correspond to valid simulations within a semiclassical framework.

Filtering at the post-processing stage was carried out as follows. The WKB procedure can be used to determine the vibrational quantum number v' on the effective potential. In general, a real, non-integer number is obtained for v'. By applying a binning criterion, only trajectories with v' within certain thresholds are retained for further analysis. This ensures that only trajectories are analyzed in which ZPE was not transformed to other forms of energy during the simulation. Three different thresholds were used here: $\text{frac}(v') = \pm 0.1$, ± 0.01, and ± 0.001, where $\text{frac}(x)$ is the difference of x to the closest integer value. These values correspond to a conservation of the ZPE within 220.70 cm^{-1}, 22.07 cm^{-1}, and 2.21 cm^{-1}, respectively.

Rotational j' states are rounded to the next closest integer value divisible by 2 in order to fulfill restrictions imposed by the symmetry of N_2^+, which can exist in either the *ortho* or *para* nuclear spin state. If a binning criterion similar to the vibrational quantum number is applied to j' states, the number of trajectories that fulfill both criteria decreases dramatically. Hence, no such binning was applied for j'. For the final state analysis of trajectories run on the corrected PES, the ZPE is added back into the classical rovibrational energy, since it was removed before generating the initial conditions.

The final distribution of j' states, $P(j')$, is determined from the WKB procedure after the complex has dissociated. An event is classified as "inelastic" if the final j' differs from the initial j'', i.e., $j' \neq j''$. As the simulations involve numerical imprecisions of about 3.5 cm^{-1} (see Figure 5, upper panel), corresponding to roughly the energy difference between $j'' = 0$ and $j' = 1$ for N_2^+ (based on a rotational constant of $B = 1.932$ cm^{-1}),[40] an additional criterion on the necessary amount of change in j' was introduced to classify inelastic transitions. For this, the quantity j^* is used. Only trajectories for which the final j' differs by more than j^* from the initial j'' state are considered to correspond to an inelastic collision.

Rotational excitation. Figure 6 reports the final state distribution $P(j')$ for N_2^+ from simulations on the bare and ZPE-corrected PES starting from $j'' = 0$. Results are presented for simulations at $T = 90$ K and $T = 300$ K. The distributions differ slightly between the two PESs while temperature has only a minor effect on $P(j')$. On the bare PES, higher j'–states are populated compared to simulations on the ZPE-corrected PES. Possibly, this is due to the more isotropic shape of the ZPE-corrected PES due to angular averaging. Also, as the well is more shallow on the ZPE-corrected PES due to inclusion of ZPE, the anisotropy near the inner wall is less accessible. The maximum of the distribution is at $j' = 2$, whereas it is at $j' = 0$ for the bare PES. This already suggests that more than a fraction (i.e., 2% in the experiments[3]) of the collisions are inelastic.

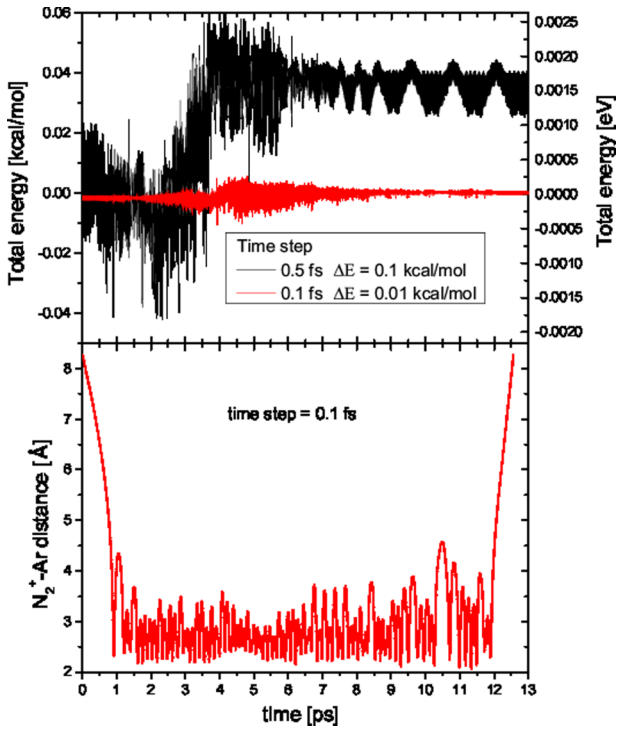

FIG. 5. A representative molecular dynamics simulation for the collision between N_2^+ and Ar. The upper panel reports the variation of the total energy as a function of time for time steps $\Delta t = 0.5$ and 0.1 fs, respectively. In the bottom panel, the distance between the ion and the incoming Ar atom is shown for $\Delta t = 0.1$ fs. After ≈0.5 ps, the complex is formed and lives for about 12.5 ps after which it breaks up again.

The distribution changes only slightly between different filtering criteria, as is shown in the inset in Figure 6. The percentage of inelastic and elastic collisions for the bare PES and a filtering criterion of $\text{frac}(v') = \pm 0.01$ are summarized in Table I. A collision is inelastic if the rotational quantum number of the diatomic differs from the initial j'' by more than j^*, i.e., $j' \notin [j'' - j^*, j'' + j^*]$. Even with an unrealistically large margin of $j^* = 4$, the fraction of inelastic collisions are well above the experimentally reported value of 2%.[3] Depending on the figure of merit j^* used, 20%–40% of collisions are inelastic, see Table I.

Figure 7 shows the correlation between impact parameter b and j' states. It is typically found that smaller impact parameters lead to higher rotational excitation whereas collisions with large b are preferentially elastic.

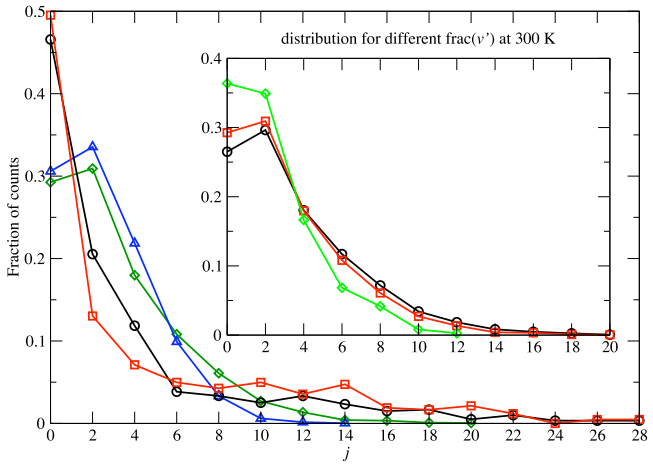

FIG. 6. Green diamonds (ZPE-corrected, 300 K), blue triangles (ZPE-corrected, 90 K), black circles (bare, 300 K), red squares (bare, 90 K). Distribution of j' states after dissociation for ZPE conservation criterion frac(v') = ±0.01 and different temperatures. Trajectories were started with an initial $j'' = 0$ and evolved on the bare and ZPE-corrected PES. The total count of trajectories that meet the conservation criterion are 4207 ($T = 300$ K) and 3309 ($T = 90$ K) on the corrected and 599 ($T = 300$ K) and 422 ($T = 90$ K) on the bare PES, respectively. Note that trajectories on the corrected PES are much more likely to meet the criterion, because ZPE is removed during the dynamics and added back in the analysis. As such, the conservation criterion on the corrected PES can only be violated by an uptake of energy, whereas it can be violated by an uptake or loss of energy on the bare PES. *Inset*: distribution of j' states after dissociation for different ZPE conservation criteria (frac(v') = ±0.1, black circles, frac(v') = ±0.01, red diamonds, frac(v') = ±0.001, green squares) at $T = 300$ K on the ZPE-corrected PES. The number of trajectories that meet the criterion are 19 821, 4207, and 745, respectively. The distribution changes slightly but shows the same overall behaviour for the different filtering criteria.

A remarkable result is that excitation to the highest rotational states is only found for trajectories with shorter lifetimes (see Figure 8). Closer examination of some individual trajectories with short lifetime shows that no tight $[N_2Ar]^+$ complex has to be formed for rotational excitation of N_2^+ to occur. A "tight complex" refers to a situation in which the collision partners come close enough to at least once entering the short-range repulsive region of the interaction potential. For rotational excitation, it is sufficient for the two collision partners to fly past each other such as to influence their respective flight paths. The interaction between N_2^+ and

TABLE I. Percentage of elastic and inelastic collisions for a filtering criterion of frac(v'') = 0.01 with initial $j = 0$. A collision is considered as inelastic when j'' changes from 0 to $j' > j^*$.

	Elastic (%)	Inelastic (%)
	Bare PES	
$T = 90$ K ($j^* = 2$)	63	37
$T = 300$ K ($j^* = 2$)	67	33
$T = 90$ K ($j^* = 4$)	70	30
$T = 300$ K ($j^* = 4$)	79	21
	ZPE-corrected PES	
$T = 90$ K ($j^* = 2$)	64	36
$T = 300$ K ($j^* = 2$)	60	40
$T = 90$ K ($j^* = 4$)	86	14
$T = 300$ K ($j^* = 4$)	78	22

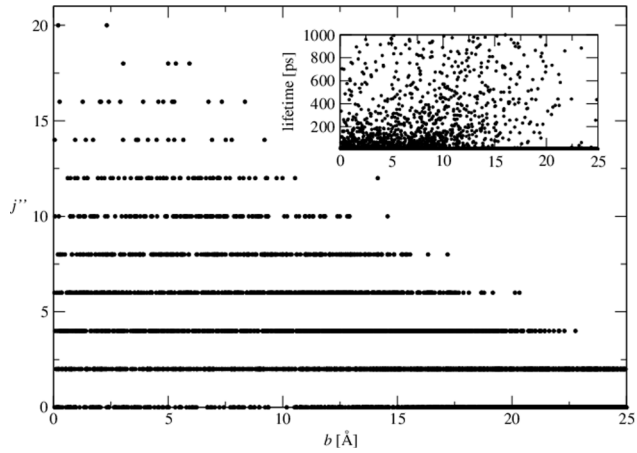

FIG. 7. Impact parameter b *vs.* j' ($j'' = 0$, $T = 300$ K) on the corrected PES. Large rotational excitation is observed only for small impact parameters. Plots for other temperatures on the corrected and bare PES show similar behaviour. Impact parameter b *vs.* lifetime. The lifetime is not correlated to the impact parameter (inset).

Ar leads to a torque which results in pronounced rotational excitation of N_2^+. Such "*fly-by*" trajectories (lifetime of the complex shorter than 5 ps) lead to excitation to higher rotational states than trajectories with a longer lifetime and make up 21.5% of all trajectories.

Counter-intuitively, the impact parameter b is not correlated to the lifetime of the complex (see inset of Figure 7). In fact, the complex can be formed and live for a very long time even for large impact parameters, provided that the collision energy is sufficiently low. Conversely, small impact parameters still sometimes lead to fly-by trajectories, provided that the collision energy is sufficiently large. It is the combination of a small impact parameter and a high collision energy (leading to fly-by trajectories) that leads to the highest rotational excitations.

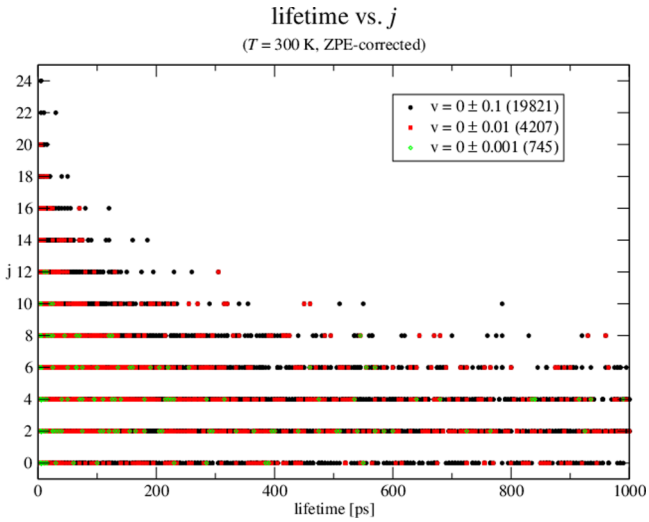

FIG. 8. Lifetime *vs.* j' ($j'' = 0$, $T = 300$ K) on the corrected PES for different ZPE conservation criteria, numbers in parentheses indicate how many trajectories meet the criterion. The largest rotational excitation is observed only for short lifetimes. Plots for other temperatures on the corrected and bare PES show similar behaviour.

The earlier experiments[3] were thermal and started from a distribution of rotational states, but the initial rotational state studied was $j'' = 6$. Hence, additional simulations were carried out for this case. 25 000 independent trajectories were started on the ZPE-corrected PES. Figure 9 shows the distribution of j' states after the complex dissociates. The percentage of inelastic collisions for the strictest filtering criterion frac(v') = ±0.001 and $j^* = 0$ are 41% and decrease to 17% for $j^* = 2$, respectively. The rate constant for rotational excitation/relaxation was calculated according to[11]

$$k(T) = \sqrt{\frac{8}{\pi\mu\beta}}\frac{2\pi b_{\max}}{g(T)N_{\text{tot}}}\sum_{i=1}^{N_{\text{reac}}} b_i, \tag{8}$$

where μ is the reduced mass of the N_2^+–Ar complex, $g(T)$ is the electronic degeneracy factor, $b_{\max}$ is the maximum impact parameter, b_i is the impact parameter of trajectory i, N_{tot} is the total number of trajectories that meet the filtering criterion, N_{reac} is the number of inelastic trajectories ($|j' - j''| > j^*$) and $\beta = 1/(k_B T)$. The calculated value of $k_{j''=6\to j'\neq 6} = 1.17 \cdot 10^{-9}$ cm^3 s^{-1} is two orders of magnitude larger than the reported value of $k = (1.4 \pm 0.4) \cdot 10^{-11}$ cm^3 s^{-1}.[3] However, it should be noted that the experimental value was not directly measured, but inferred from a kinetic model based on the rate coefficient for charge transfer and the rate of laser excitation.

Since the Langevin rate is often considered to be an upper bound for reaction rates, it is surprising that the *computationally determined* rate $k_{j''=6\to j'\neq 6}$ is about 60% larger than the Langevin rate $k_L = 7.4 \cdot 10^{-10}$ cm^3 s^{-1}.[3] However, rates larger than k_L have been reported previously in the literature.[41] It should be noted that Langevin theory assumes an idealized form for the centrifugally corrected interaction potential between the ion, which is modelled as a point charge, and the neutral atom given by[42]

$$V_L(R) = \frac{1}{2}\frac{L^2}{\mu R^2} - \frac{\alpha' e^2}{8\pi\epsilon_o R^4}, \tag{9}$$

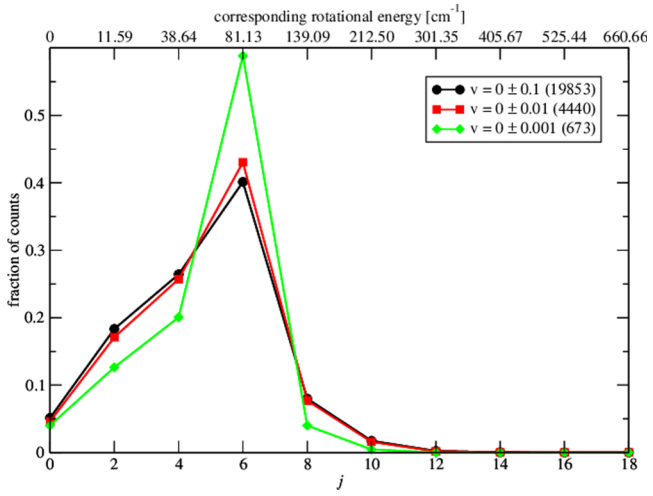

FIG. 9. Distribution of j' states after dissociation for different ZPE conservation criteria at $T = 90$ K. The numbers in brackets show how many trajectories meet the criterion. For every value of j, the corresponding rotational energy is given (the rotational constant is $B = 1.932$ cm^{-1}).[40] Trajectories were started with an initial $j'' = 6$ and evolved on the ZPE-corrected PES.

where $L = \mu v b$, v is the relative collision velocity, α' the polarizability volume of the neutral species, μ the reduced mass, b the impact parameter, and R the distance between centre of mass of the molecular ion and neutral species. A comparison between the $1/R^4$ term in Eq. (9) and the actual interaction potential shows that Langevin theory is insufficient to describe the collisional rate. In particular, the true PES decays more slowly to zero and the anisotropy of the PES (see Figure 3), which is crucial for the dynamics, is completely neglected in the Langevin model. Nonetheless, if Langevin theory is applied naively to the same set of trajectories that was used to calculate the $k_{j''=6\to j'\neq 6}$ rate and Eq. (8) is used to calculate a rate (counting those trajectories as "reactive" that satisfy $E_C \geq V_L(R_{\max})$, where E_C is the collision energy and $V_L(R_{\max})$ is the Langevin interaction potential at the position of the maximum of the centrifugal barrier according to Langevin theory), a rate constant of $k_L = 6.2 \cdot 10^{-10}$ cm^3 s^{-1} is obtained. This is in good agreement with the value of $k_L = 7.4 \cdot 10^{-10}$ cm^3 s^{-1} from Langevin theory. Note however that this analysis can be performed from the initial conditions without running actual dynamics and merely shows that the initial conditions for our simulations are consistent with the Langevin model. However, the model itself is insufficient to describe the actual dynamics. It should also be considered that k_L measures merely a sort of "collision rate," but as was pointed out earlier, the complex does not need to be formed in order for rotational relaxation or excitation to occur. In fact, for 92.4% of the trajectories, the Langevin model correctly predicts whether the complex is formed or not from just the initial conditions. Since the observed rate is 60% larger than the Langevin rate, this further indicates that rotational excitation can occur without complex formation. A final test was to run simulations with an explicitly isotropic PES beyond 8 Å. At this distance, the PES is still appreciably anisotropic (≈50 cm^{-1} between linear and T-shape geometries). Hence, the PES was multiplied by an empirical factor of exp(−(R/7.3 Å)^{20}), which ensures a smooth cutoff at long-range, yet leaving the short-range part of the PES largely unaffected. Although this PES fulfills the requirement of Langevin theory, namely, that the long range part of the PES should be isotropic, the computed rate is unaffected and still exceeds the Langevin rate. It is suspected that the anisotropy in the range below 8 Å is the main cause for rotational excitation.

IV. CONCLUSION

Quasi-classical molecular dynamics simulations of the nonreactive collision between the N_2^+ cation and Ar atoms at two different temperatures show that inelastic rotational excitation of the ion in the product channel is important and occurs more frequently than previously assumed. The simulations use an RKHS PES based on UCCSD(T)/aug-cc-pVTZ electronic structure calculations and correct handling of the asymptotics within the RKHS framework. Analysis of the results for $j'' = 6$ using a strict filtering criterion of frac(v') = ±0.001 and a figure-of-merit $j^* = 2$ suggests that inelastic collisions occur in at least 17% of the cases which is one order of magnitude larger than

reported in earlier experiments (2%).[3] However, it cannot be ruled out that subtle quantum mechanical effects affect the quantitative conclusions of the present work. Converged close-coupling calculations using the present PES will be a desirable complement to the present considerations, but challenging due to the deep well and the large anisotropy of the PES.

Interestingly, the $[N_2Ar]^+$ complex does not need to be formed (and stabilized) for rotational excitation to occur. A sufficiently close encounter of the two collision partners is sufficient to mutually influence their flight paths and lead to rotational excitation. It should be pointed out that the PES used in this work was calculated using a single-reference method. Electronic effects, which are not adequately captured using single-reference methods, might play a non-negligible role in the dissociative region of the PES. Further investigations should employ multi-reference methods such as multireference configuration interaction to capture electronic effects which are, however, outside the scope of the present work. For a complete understanding of the rate of rotational excitation in the N_2^+–Ar system, new experiments which allow precise control of the exact quantum state of the collision partners and additional computational investigations are necessary.

ACKNOWLEDGMENTS

The authors thank S. Willitsch for discussions. Part of this work was supported by the United State Department of the Air Force which is gratefully acknowledged (to J.C.C.-P.). Support by the Swiss National Science Foundation through Grant Nos. 200021 and 117810, the NCCR MUST (to M.M.), and the University of Basel is also acknowledged.

[1]C. Myatt, E. Burt, R. Ghrist, E. Cornell, and C. Wieman, Phys. Rev. Lett. **78**, 586 (1997).
[2]M. S. Elioff, J. J. Valentini, and D. W. Chandler, Science **302**, 1940–1943 (2003).
[3]S. Schlemmer, T. Kuhn, E. Lescop, and D. Gerlich, Int. J. Mass Spect. **185–187**, 589–602 (1999).
[4]J. C. Grieman, J. T. Hansen, and J. Moseley, Chem. Phys. Lett. **85**, 53–56 (1982).
[5]R. Candori, S. Cavalli, F. Pirani, A. Volpi, D. Cappelletti, P. Tosi, and D. Bassi, J. Chem. Phys. **115**, 8888–8898 (2001).
[6]H. H. Teng and D. Conway, J. Chem. Phys. **59**, 2316–2323 (1973).
[7]R. H. Schultz and P. Armentrout, Chem. Phys. Lett. **179**, 429–434 (1991).
[8]S. Kato, J. A. de Gouw, C.-D. Lin, V. M. Bierbaum, and S. R. Leone, Chem. Phys. Lett. **256**, 305–311 (1996).
[9]M. Germann, X. Tong, and S. Willitsch, Nat. Phys. **10**, 820–824 (2014).
[10]X. Tong, T. Nagy, J. Y. Reyes, M. Germann, M. Meuwly, and S. Willitsch, Chem. Phys. Lett. **547**, 1–8 (2012).
[11]J. Castro-Palacio, T. Nagy, R. Bemish, and M. Meuwly, J. Chem. Phys. **141**, 164319 (2014).
[12]J. Castro-Palacio, R. Bemish, and M. Meuwly, J. Chem. Phys. **142**, 091104 (2015).
[13]T.-S. Ho, T. Hollebeek, H. Rabitz, L. B. Harding, and G. C. Schatz, J. Chem. Phys. **105**, 10472–10486 (1996).
[14]J. Lim, M. D. Frye, J. M. Hutson, and M. R. Tarbutt, Phys. Rev. A **92**, 053419 (2015).
[15]G. Czakó and J. M. Bowman, Proc. Natl. Acad. Sci. U. S. A. **109**, 7997–8001 (2012).
[16]A. G. de Oliveira-Filho, F. R. Ornellas, and J. M. Bowman, J. Phys. Chem. Lett. **5**, 706–712 (2014).
[17]A. N. Panda, D. Herraez-Aguilar, P. G. Jambrina, J. Aldegunde, S. C. Althorpe, and F. Javier Aoiz, Phys. Chem. Chem. Phys. **14**, 13067–13075 (2012).
[18]T. D. Sewell, D. L. Thompson, J. D. Gezelter, and W. H. Miller, Chem. Phys. Lett. **193**, 512–517 (1992).
[19]A. Varandas, Chem. Phys. Lett. **439**, 386–392 (2007).
[20]J. M. Bowman, B. Gazdy, and Q. Sun, J. Chem. Phys. **91**, 2859–2862 (1989).
[21]G. Czakó, A. L. Kaledin, and J. M. Bowman, Chem. Phys. Lett. **500**, 217–222 (2010).
[22]T. Hollebeek, T.-S. Ho, and H. Rabitz, Annu. Rev. Phys. Chem. **50**, 537–570 (1999).
[23]T. Hollebeek, T.-K. Ho, and H. Rabitz, J. Chem. Phys. **106**, 7223 (1997).
[24]T. H. Dunning, Jr., J. Chem. Phys. **90**, 1007–1023 (1989).
[25]D. E. Woon and T. H. Dunning, Jr., J. Chem. Phys. **98**, 1358–1371 (1993).
[26]M. J. Frisch *et al.*, Gaussian 09, Revision A.02, Gaussian, Inc., Wallingford, CT, 2009.
[27]M. Meuwly and J. M. Hutson, J. Chem. Phys. **110**, 3418–3427 (1999).
[28]R. B. Singh and D. K. Rai, J. Mol. Spec. **19**, 424–434 (1966).
[29]J. Mähnert, H. Baumgärtel, and K.-M. Weitzel, J. Chem. Phys. **102**, 180–188 (1995).
[30]T. Ho and H. Rabitz, J. Chem. Phys. **104**, 2584–2597 (1996).
[31]G. H. Golub and C. F. van Loan, *Matrix Computations* (The Johns Hopkins University Press, Baltimore, London, 1983).
[32]P. Soldan and J. M. Hutson, J. Chem. Phys. **112**, 4415–4416 (2000).
[33]D. Xie, C. Xu, T.-K. Ho, H. G. L. Rabitz, S. Y. Lin, and H. Guo, J. Chem. Phys. **126**, 074315 (2007).
[34]H.-G. Yu and G. Nyman, J. Chem. Phys. **111**, 6693–6704 (1999).
[35]B. R. Brooks *et al.*, J. Chem. Comp. **30**, 1545–1614 (2009).
[36]M. Abramowitz and I. A. Stegun, *Handbook of Mathematical Functions: with Formulas, Graphs, and Mathematical Tables* (Courier Corporation, 1964).
[37]R. N. Porter, L. M. Raff, and W. H. Miller, J. Chem. Phys. **63**, 2214–2218 (1975).
[38]R. L. Liboff, *Introductory Quantum Mechanics*, 4th ed. (Addison-Wesley, Massachusetts, 2003).
[39]J. Peterson, A. Le Padellec, H. Danared, G. Dunn, M. Larsson, A. Larson, R. Peverall, C. Strömholm, S. Rosén, and M. Af Ugglas, J. Chem. Phys. **108**, 1978–1988 (1998).
[40]E. Colbourn and A. Douglas, J. Mol. Spec. **65**, 332–333 (1977).
[41]S. Andersson, Ç Barinovs, and G. Nyman, ApJ **678**, 1042 (2008).
[42]B. R. Eichelberger, T. P. Snow, and V. M. Bierbaum, J. Am. Soc. Mass Spec. **14**, 501–505 (2003).